Environ Monit Assess (2015) 187: 641
DOI 10.1007/s10661-015-4847-1

Accuracy assessment of land cover/land use classifiers in dry and humid areas of Iran

Saleh Yousefi · Reza Khatami · Giorgos Mountrakis · Somayeh Mirzaee · Hamid Reza Pourghasemi · Mehdi Tazeh

Received: 27 April 2015 / Accepted: 4 September 2015 / Published online: 24 September 2015

Abstract Land cover/land use (LCLU) maps are essential inputs for environmental analysis. Remote sensing provides an opportunity to construct LCLU maps of large geographic areas in a timely fashion. Knowing the most accurate classification method to produce LCLU maps based on site characteristics is necessary for the environment managers. The aim of this research is to examine the performance of various classification algorithms for LCLU mapping in dry and humid climates (from June to August). Testing is performed in three case studies from each of the two climates in Iran. The reference dataset of each image was randomly selected from the entire images and was randomly divided into training and validation set. Training sets included 400 pixels, and validation sets included 200 pixels of each LCLU. Results indicate that the support vector machine (SVM) and neural network methods can achieve higher overall accuracy (86.7 and 86.6 %) than other examined algorithms, with a slight advantage for the SVM. Dry areas exhibit higher classification difficulty as man-made features often have overlapping spectral responses to soil. A further observation is that spatial segregation and lower mixture of LCLU classes can increase classification overall accuracy.

Keywords Humid and dry areas · Classification accuracy · SVM · Neural networks · Land cover/land use

S. Yousefi
Watershed Science Department, Faculty of Natural Resources, Tarbiat Modares University (TMU), Mazandaran, Iran

R. Khatami · G. Mountrakis
Department of Environmental Resources Engineering, State University of New York College of Environmental Science and Forestry, One Forestry Drive, Syracuse, NY 13210, USA

S. Mirzaee
College of Natural Resources, Lorestan University, Lorestan, Iran

H. R. Pourghasemi (✉)
Department of Natural Resources and Environmental Engineering, College of Agriculture, Shiraz University, Shiraz, Iran
e-mail: hamidreza.pourghasemi@yahoo.com

H. R. Pourghasemi
e-mail: hr.pourghasemi@shirazu.ac.ir

M. Tazeh
College of Natural Resources, Ardekan University, Ardekan, Iran

Introduction

Information on land cover/land use (LCLU) plays a key role in natural resource management (Wentz et al. 2006; Soffianian and Madanian 2015; Wang et al. 2015). LCLU maps are preliminary inputs for planning and modeling ecosystem activities (Kennaway et al. 2008; Martinuzzi et al. 2009; Shaw et al. 2014; Bhattarai et al. 2015). LCLU mapping using satellite images has become widely popular in the last decades (Van Der Linden et al. 2007; Chen et al. 2009; Neuenschwander et al. 2009; Jacqueminet et al. 2013; Vorovencii 2014a; Mohammady et al. 2015; Sakizadeh 2015; Sen et al. 2015; Soffianian and Madanian 2015).

Numerous researches have been published on comparison of different remote sensing image classification algorithms used for LCLU mapping (De Moraes et al.

1998; Wentz et al. 2006; Dixon and Candade 2008; Khatami and Mountrakis 2012; Vorovencii 2014b). However, there has not yet been a direct comparison evaluating the performance of common classification algorithms in humid and dry regions for LCLU mapping. This is the objective of our work. These studies are important as minor changes in dry and humid ecosystems can result in significant alterations in domain tolerances of flora and fauna (Walker and Schulze 2008). Moreover, when large human populations live in regions with humid and dry climate, the natural resources of those areas can be under population stress and overuse (Vörösmarty et al. 2000; Núñez et al. 2002).

Materials and methods

Study area

Shahreza in Isfahan Province, Taft in Yazd Province, and Zarand in Kerman Province, located in central part of Iran, were selected as dry climate. While Kordkoi in Golestan Province, Noor in Mazandaran Province, and Talesh in Guilan Province, located in the northern part of Iran, were selected as humid climate (Fig. 1 and Table 1). Figure 2 shows the steps of the methodology applied in the current study in order to investigate the accuracy of land cover/ land use classifiers.

Materials

Three Landsat 7 ETM+ scenes from the dry and three from the humid climates were included in this study. At first, for solving of the scan line corrector (SLC) failure of images, a simple and effective gap-fill method developed by the US Geological Survey was applied (USGS 2004; Mohammady et al. 2014). In the next step, geometric correction of the Landsat images was done using 25 control points extracted from existing 1:25,000 topographic maps with RMSE between 0.18 and 0.22 pixels. In addition, only the six 30-m reflective bands of Landsat images were used. Reference datasets for image classification and accuracy assessment were constructed using topographic maps and field visits. Simple random sampling was used to sample the reference dataset. For each land cover, 600 pixels were identified. For the humid climate, the LCLU classes were forest, residential, and agriculture areas. For the dry climate, the LCLU classes were desert, residential, and agriculture. The reference dataset of each image was randomly divided into training and validation set. Training sets included 400 pixels of each land cover and were used for image classification. Validation sets included 200 pixels of each land cover and were used for classification accuracy assessment.

Algorithmic selection and setup

The performance of five common classification algorithms was examined. These algorithms include maximum likelihood (ML), minimum distance to mean (MDM), Mahalanobis distance (MD), neural network (NN), and support vector machine (SVM). All six Landsat images are classified by the five classifiers using the same training dataset per case study.

ML is one of the most common parametric algorithms for image classification (Jensen 1996; Chen et al. 2011). This algorithm is based on Bayes theory in which the posterior probability that a pixel belongs to a class is calculated for all classes and the pixel is assigned to the most likely one (Pfanzagl 1994). In MDM algorithm, first, the mean value for each band is calculated for all classes; then, each pixel is allocated to the class with the nearest mean in that feature space (Richards and Jia 2006; Ghimire and Wang 2012). MD algorithm is similar to MDM in that the distance from mean values obtained from training data is the measure for class allocation (Xing et al. 2003; Zhang et al. 2011).

NN is a nonparametric algorithm that does not make any assumptions on the distribution of data (Foody 2004; Lu and Weng 2007; Dixon and Candade 2008). One challenge in using NN classifiers is to decide the appropriate network architecture and training parameters. In our study, different combinations of network values were tested and the classification with the highest overall accuracy was determined for each case study. The optimized network parameters include training threshold contribution, tested with three values of 0.5, 0.7, and 0.9; training rate, tested with three values of 0.1, 0.2, and 0.5; training momentum, tested with four values of 0.1, 0.2, 0.5, and 0.9; structure of hidden layers 1 and 2; and a fixed logistic activation function. All combinations of the above parameters are run for 1000 training iterations, and optimal combination is selected based on overall accuracy of classifications.

SVM is a more recent advanced classification algorithm which is widely used for LCLU mapping (Huang et al. 2002; Mountrakis et al. 2011). The idea

Fig. 1 Geographic location of case studies in Iran

of SVM is to find the optimal hyperplanes that separate target classes with minimum misclassification error. Similar to NN, in our implementation, different parameter values were tested to find the optimal values for each image. Initially, seven values for the gamma parameter in kernel function including 1000, 100, 10, 1, 0.1, 0.01, and 0.001 and seven values for the penalty parameter including 1000, 100, 10, 1, 0.1, 0.01, and 0.001 were tested. After determination of the approximate range of optimal value for the two parameters, additional values were tested for further fine tuning. For all SVM classifications, the radial basis function (RBF) was used as the kernel function.

Table 1 Summary information of case studies

Climate	Case study	Area (Ha)	Average annual precipitation (mm)	Landsat image date
Humid	Kordkoi	11,358	970	08.29.2006
	Noor	8919	1030	07.19.2006
	Talesh	10,761	1130	08.15.2005
Dry	Shahreza	9560	140	06.10.2006
	Taft	9198	164	08.06.2006
	Zarand	10,761	111	08.05.2005

Statistical analysis

Analysis of variance (ANOVA) is used for statistical comparison of classification algorithms (Fisher 1926). ANOVA is a statistical tool to compare different categories. It is similar to *t* test, but it is done when more than two categories are compared at the same time. In an ANOVA, the total sum of squares is partitioned into between-groups sum of squares or the portion that can be explained by treatments, i.e., classification algorithms here, and within-groups sum of squares or the portion that is considered as random error. In this study, the experimental design is randomized complete block design (RCBD) with images as blocks, as classification methods are implemented on the same images (as opposed to completely randomized design (CRD) in which samples, i.e., images here, for each method are independent from other methods). Therefore, the within-groups sum of squares is itself partitioned into the portions that can be attributed to variation among images and random error. SAS software is used for ANOVA implementation.

In order to specify which classifiers are different, pairwise Tukey's honestly significant difference (HSD) tests were used to compare method means. Tukey's HSD test is similar to *t* test, but it is used when a large number of pairwise comparisons are to be done. It helps

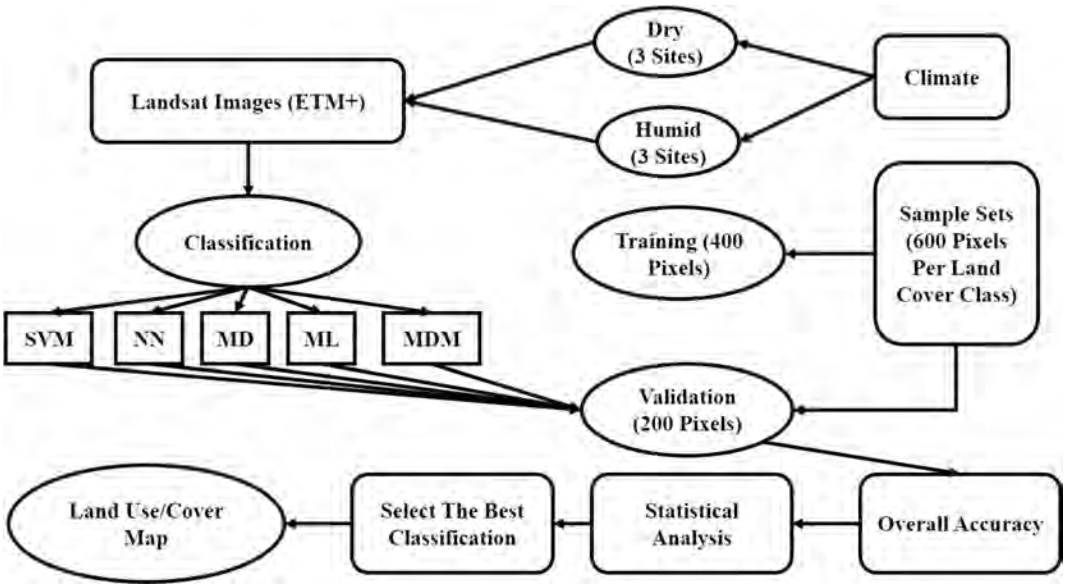

Fig. 2 Flow chart of the methodology adopted in LCLU classification and accuracy assessment

to control experimentwise error rate, i.e., the probability that at least for one comparison, the null hypothesis is rejected falsely, at desired level.

Results

Based on De Martonne climate categorization (De Martonne 1926) and using the average annual precipitation, three case studies in the north have humid climate and the three case studies in the central part of Iran have dry climate.

The optimal classifier parameter values for NN and SVM are obtained by implementing all combinations of the aforementioned parameter values for the six case studies. Table 2 shows the values that result in the highest overall accuracy for NN and SVM classifiers. Accuracy assessment of different classifications is undertaken using the same validation dataset for each image. The results are presented in two sections of independent assessment of classifier performance and statistical comparison of classifiers.

Independent assessment of classifier performance

Tables 3 and 4 present user's accuracy, producer's accuracy, and overall accuracy independent of class probability as our focus is classifier performance that is not site-specific (Stehman 1997; Foody 2002). Results are presented for the classification of humid and dry case studies, respectively.

Figures 3 and 4 show the classified maps for Kordkoi and Shahreza case studies from humid and dry climates, respectively. In Fig. 3, forested areas are mapped very similarly for all classifiers. This is also evident in the user and producer accuracies of forest class for all classifiers (Table 3).

Statistical comparison of classifiers

Three ANOVAs are done to compare the overall accuracies of the five classifier families: one for humid climate, one for dry climate, and one for the two climates combined. Table 5 shows the ANOVA results. The null hypothesis is that the five classifiers have the same overall accuracy, and the alternative hypothesis is that at least two classifiers have different overall accuracies. As Table 5 shows, for all three ANOVAs, the sum of squares explained by classification methods, which indicates variation among average overall accuracy of methods, is significantly larger than that of the error (α=0.05). This implies that differences among classification algorithms are not just a matter of random error. Consequently, the p values of all three ANOVAs are significantly small which suggests that at least two classifiers have different performance for all three cases. In addition, the sum of squares explained by

Table 2 Neural network and SVM optimal parameter values

Climate	Case study	Neural network				SVM	
		Training threshold contribution	Training rate	Training momentum	Number of hidden layers	Penalty parameter	Gamma
Humid	Kordkoi	0.5	0.2	0.9	1	100	0.167
	Noor	0.9	0.1	0.9	2	100	0.167
	Talesh	0.5	0.1	0.9	2	250	0.167
Dry	Shahreza	0.7	0.1	0.5	1	550	0.167
	Taft	0.5	0.2	0.9	1	850	0.167
	Zarand	0.7	0.1	0.9	2	25	0.167

case studies, which indicates variation among average overall accuracy of images, is considerably large compared to that of the error (786.89 vs. 341.14). This indicates that the blocking experimental design used in this research was efficient to obtain smaller mean square errors.

Table 6 presents mean overall accuracy of classifiers and the results of pairwise comparisons between them. In both climates, SVM and NN outperformed the other classifiers with an obvious margin. Each of the SVM and NN classifiers performs the best in one climate, and SVM performs the best when two climates are aggregated. MD and ML classifiers form another group at the middle, and MDM has the lowest overall accuracy for both climates. For each climate, the difference between the means sharing the same letter is not statistically significant at the 0.05 significance level. For example, in humid climate, the difference between SVM and NN is not statistically significant as they share the superscript “a,” but the difference between SVM and MD is significant. Small sample size for each climate (three images per climate)

Table 3 Accuracy measures of classification algorithms for humid case studies

Case study	Classifier	Rank of OA	Agriculture		Forest		Residential		OA (%)
			UA (%)	PA (%)	UA (%)	PA (%)	UA (%)	PA (%)	
Kordkoi	SVM	1	88.6	95.7	98.6	100.0	96.4	87.4	94.3
	NN	2	88.7	93.8	97.2	100.0	94.9	86.9	93.5
	MD	3	84.7	91.9	97.1	98.5	93.8	84.6	91.6
	ML	4	85.5	84.3	96.7	100.0	86.7	85.1	89.7
	MDM	5	87.5	70.0	95.8	100.0	76.9	88.8	86.2
Noor	SVM	1	83.3	87.6	93.2	91.9	88.6	85.2	88.2
	NN	2	80.8	88.9	95.5	90.9	89.3	84.2	88.0
	MD	4	78.6	81.1	85.2	90.9	88.3	79.4	83.8
	ML	3	76.7	86.6	94.4	89.5	85.4	78.5	84.9
	MDM	5	77.1	74.7	82.3	91.4	86.5	79.9	81.9
Talesh	SVM	1	86.2	87.4	93.4	88.5	86.6	89.9	88.6
	NN	2	85.2	85.6	94.8	87.0	83.0	89.4	87.3
	MD	3	85.2	82.8	87.7	88.9	85.8	87.0	86.2
	ML	4	85.7	83.3	90.1	87.5	82.7	87.5	86.1
	MDM	5	89.8	75.4	85.2	85.6	83.1	87.5	82.7

UA user’s accuracy, *PA* producer’s accuracy, *OA* overall accuracy

Table 4 Accuracy measures of classification algorithms for dry case studies

Case study	Classifier	Rank of OA	Agriculture		Desert		Residential		OA (%)
			UA (%)	PA (%)	UA (%)	PA (%)	UA (%)	PA (%)	
Shahreza	SVM	2	85.0	90.6	93.9	85.4	85.5	87.0	87.7
	NN	1	86.4	89.2	88.7	91.4	89.7	84.3	88.2
	MD	3	82.5	84.0	90.2	83.8	81.9	85.7	84.5
	ML	4	79.5	76.1	82.1	90.4	81.6	86.1	84.1
	MDM	5	57.2	48.4	56.7	83.8	63.6	45.4	58.5
Taft	SVM	1	76.7	87.4	91.8	81.1	77.1	74.5	81.1
	NN	2	76.2	87.8	95.3	79.1	74.7	75.0	80.8
	MD	4	78.6	77.9	91.1	79.1	68.9	78.3	78.4
	ML	3	78.1	78.8	90.8	81.1	70.7	77.4	79.1
	MDM	5	76.6	76.6	65.0	76.7	59.4	49.1	67.5
Zarand	SVM	2	89.3	78.9	77.8	84.1	75.0	78.2	80.4
	NN	1	88.0	82.1	83.1	82.7	74.5	80.1	81.6
	MD	4	90.7	74.0	69.0	84.6	76.6	74.4	77.6
	ML	3	86.6	78.5	75.3	89.4	79.3	72.5	80.1
	MDM	5	74.4	65.0	69.9	52.4	53.6	73.9	63.9

UA user's accuracy, *PA* producer's accuracy, *OA* overall accuracy

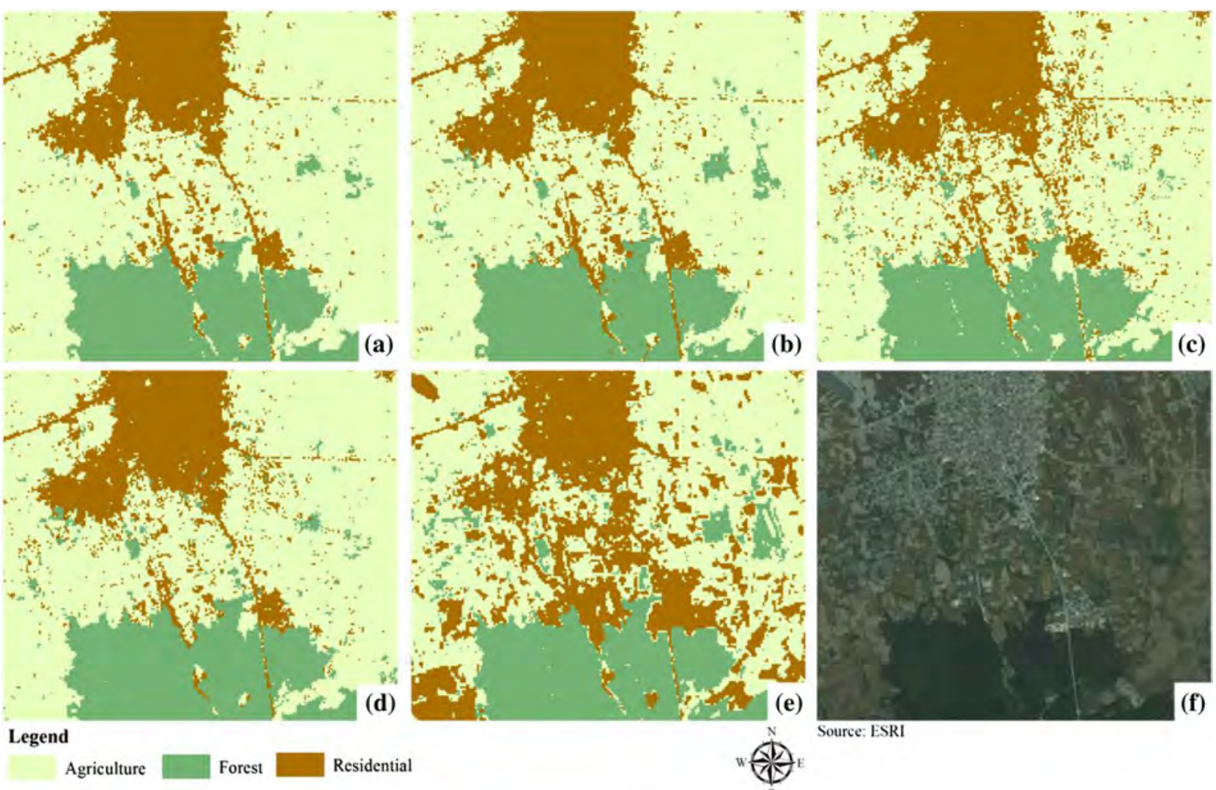

Fig. 3 Classified maps and base imagery of Kordkoi case study: **a** SVM, **b** NN, **c** ML, **d** MD, **e** MDM, and **f** high-resolution imagery

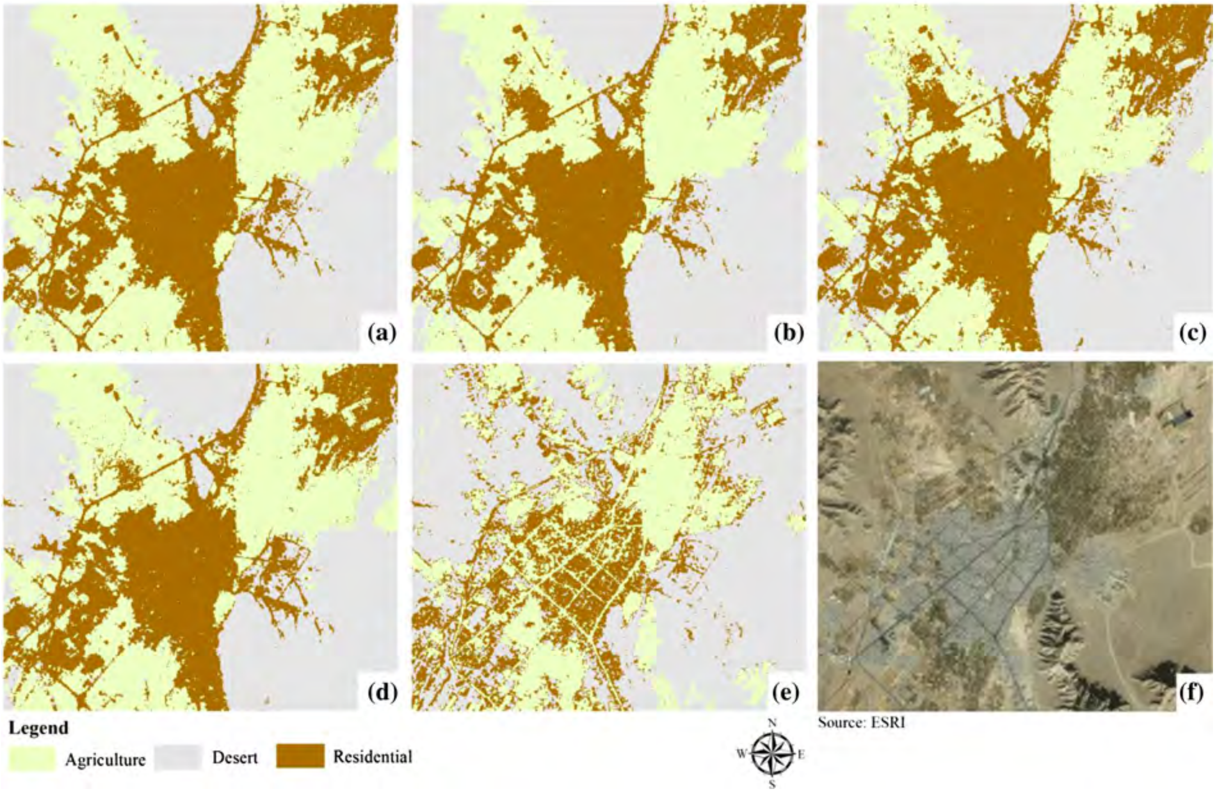

Fig. 4 Classified maps and base imagery of Shahreza case study: **a** SVM, **b** NN, **c** ML, **d** MD, **e** MDM, and **f** high-resolution imagery

resulted in finding less significant differences. It is because of substantial workload associated with incorporating additional case studies. Consequently, the power of the test is low which translates into small differences not spotted as statistically significant.

Discussions and conclusion

In this research, different classification algorithms are examined for dry and humid LCLU classification. The SVM and neural network methods performed better than

Table 5 ANOVA of overall accuracy of classification algorithms

Climate	Source of variation	Sum of squares	Degree of freedom	Mean square	*P* value
Humid	Case study	94.55	2	47.27	
	Classification algorithm	84.92	4	21.23	0.0001
	Error	6.24	8	0.78	
	Corrected total	185.72	14		
Dry	Case study	43.65	2	21.82	
	Classification algorithm	858.74	4	214.68	0.0007
	Error	105.60	8	13.20	
	Corrected total	1007.99	14		
Dry and humid	Case study	786.89	5	157.37	
	Classification algorithm	714.36	4	178.59	0.0001
	Error	341.14	20	17.05	
	Corrected total	1842.40	29		

Table 6 Tukey's HSD pairwise mean comparison

Climate	SVM	NN	MD	ML	MDM
Humid	90.4[a]	89.6[ab]	87.2[bc]	86.9[c]	83.6[d]
Dry	83.1[e]	83.6[e]	80.2[e]	81.1[e]	63.3[f]
Dry and humid	86.7[g]	86.6[g]	83.7[g]	84.0[g]	73.4[h]

[a,c,d,e,f,g,h] Are in a group and haven't any significant difference

[ab,bc] Have significant differences

other classifiers with a slight outperformance of SVM (86.7 %) over NN (86.6 %). Results of this study confirm the results of Huang et al. (2002), Oommen et al. (2008), and Szuster et al. (2011). From the algorithmic perspective, results indicate that for all three case studies in humid climate, the SVM method is the most accurate classifier in terms of classification overall accuracy. For two dry climate case studies: Shahreza and Zarand, the NN is the most accurate classifier, and in Taft, SVM is the most accurate one. However, the difference in overall accuracies between SVM and NN for all six case studies is less than 1.3 %. MD and ML are the next classifiers with similar performance. For all six case studies, MDM has the least overall accuracy among all algorithms.

One of the advantages of the SVM algorithm for land cover mapping is producing highly accurate classified images from small training sets (Mantero et al. 2005; Halder et al. 2011; Mountrakis et al. 2011). This advantage helps environmental and natural resource managers to provide LCLU maps with accurate information quickly, thus saving them time and cost (Mountrakis et al. 2011). Mahalanobis distance (83.7 %) and maximum likelihood (84.0 %) classifiers had reasonably acceptable accuracy and are advised to be used when advanced classifiers are not available. In MD, first, the covariance matrix of each class is constructed using training data. Then, the distances from an unknown pixel to all classes are normalized and used as classification measure. In other words, it counts for unequal variances of class's distribution and correlations between bands or dimensions of classification feature space. The major assumption of ML is normal distribution of pixels of each class (Xing et al. 2003; Zhang et al. 2011). Minimum distance to mean had the lowest accuracy (73.4 %) with significant distance from other classifiers. In terms of implementation, SVM and neural network require examination of different network architecture parameter values to determine the optimum values. Recent studies demonstrated that SVM performs better than many other algorithms especially when small number of training data is available (Gualtieri and Cromp 1999; Halder et al. 2011). NN has the ability to implement nonlinear classification boundaries (Kavzoglu and Mather 2003). In some case studies of this paper, the difference between the highest and the lowest overall accuracy obtained from the examined parameter values were as high as 30 %. It is even higher than the effect of classification algorithm selection.

The misclassification was more evident for the MDM classifier and to some extent for the ML classifier. Consequently, producer accuracy of residential classifier for MDM (88.8 %) is higher than all other classifiers as classification is biased toward residential class. On the other hand, the user accuracy of this class is the lowest for MDM (76.9 %) as many pixels classified as residential class are actually agriculture. With the same reasoning, low producer and high user accuracies of the agriculture class are expected for the MDM classifier. The mixture between residential and agriculture classes can be attributed to the spectral reflectance mixture of residential and soil materials. Similar mixture of classes can be seen in the Shahreza case study maps where some deserted areas are mapped as residential. This misclassification is obvious at the upper right corner of the maps. Surprisingly, the MDM-generated map look better for that area; however, the mixture between residential and agriculture classes is the worst for this classifier. Generally, the spectral reflectance mixture is stronger for the classes in dry climate compared to that of humid climate.

As a result, on average, the overall accuracies of humid climate maps are higher than those of dry climate. The user's and producer's accuracy of the residential class in many classifications is lower than that of the other classes as the spectral reflectance of the residential class mixes with soil (desert and maybe agriculture classes) (Luo and Mountrakis 2011; Mountrakis and Luo 2011). An interesting observation was that the Kordkoi case study in humid climate and Shahreza case study in dry climate had significantly higher overall accuracy than that of other case studies in their corresponding climates. This can be attributed to the spatial distribution and mixture of land covers. In these two case studies, different land covers are spatially segregated and less mixture of classes is observed.

Acknowledgments The authors would like to thank Matthieu Molinier for his valuable suggestions during writing and development of this manuscript. Also, the authors would like to thank the editorial comments and anonymous reviewers for their helpful comments on the previous version of the manuscript.

References

Bhattarai, N., Quackenbush, L. J., Dougherty, M., & Marzen, L. J. (2015). A simple Landsat–MODIS fusion approach for monitoring seasonal evapotranspiration at 30 m spatial resolution. *International Journal of Remote Sensing, 36*(1), 115–143.

Chen, H., Chang, N., Yu, R., & Huang, Y. (2009). Urban land use and land cover classification using the neural-fuzzy inference approach with Formosat-2 data. *Journal of Applied Remote Sensing*, 3(1), doi:10.1117/1.3265995.

Chen, C., Son, N., Chen, C., & Chang, L. (2011). Wavelet filtering of time-series moderate resolution imaging spectroradiometer data for rice crop mapping using support vector machines and maximum likelihood classifier. *Journal of Applied Remote Sensing*, *5*(1), 053525-053525-15.

De Martonne, E. (1926). In *Une Nouvelle fonction climatologique. L'Indice d'aridité* (pp. 449–458). Paris: Impr. Gauthier-Villars.

De Moraes, J. F. L., Seyler, F., Cerri, C. C., & Volkoff, B. (1998). Land cover mapping and carbon pools estimates in Rondonia, Brazil. *International Journal of Remote Sensing, 19*(5), 921–934.

Dixon, B., & Candade, N. (2008). Multispectral land use classification using neural networks and support vector machines: one or the other, or both? *International Journal of Remote Sensing, 29*(4), 1185–1206.

Fisher, R. A. (1926). The arrangement of field experiments. *Journal of the Ministry of Agriculture of Great Britain, 33*, 503–513.

Foody, G. M. (2002). Status of land cover classification accuracy assessment. *Remote Sensing of Environment, 80*(1), 185–201.

Foody, G. M. (2004). Thematic map comparison: evaluating the statistical significance of differences in classification accuracy. *Photogrammetric Engineering and Remote Sensing, 70*(5), 627–633.

Ghimire, S., & Wang, H. (2012). Classification of image pixels based on minimum distance and hypothesis testing. *Computational Statistics and Data Analysis, 56*(7), 2273–2287.

Gualtieri, J. A., & Cromp, R. F. (1999). Support vector machines for hyperspectral remote sensing classification. *Proceedings of SPIE - The International Society for Optical Engineering, 3584*, 221–232.

Halder, A., Ghosh, A., & Ghosh, S. (2011). Supervised and unsupervised land use map generation from remotely sensed images using ant based systems. *Applied Soft Computing Journal, 11*(8), 5770–5781.

Huang, C., Davis, L. S., & Townshend, J. R. G. (2002). An assessment of support vector machines for land cover classification. *International Journal of Remote Sensing, 23*(4), 725–749.

Jacqueminet, C., Kermadi, S., Michel, K., Béal, D., Gagnage, M., Branger, F., Jankowfsky, S., & Braud, I. (2013). Land cover mapping using aerial and VHR satellite images for distributed hydrological modelling of peri-urban catchments: application to the Yzeron catchment (Lyon, France). *Journal of Hydrology, 485*, 68–83.

Jensen, J. R. (1996). Introductory digital image processing: a remote sensing perspective. *Introductory digital image processing: a remote sensing perspective. Second edition*.

Kavzoglu, T., & Mather, P. M. (2003). The use of back propagating artificial neural networks in land cover classification. *International Journal of Remote Sensing, 24*(23), 4907–4938.

Kennaway, T. A., Helmer, E. H., Lefsky, M. A., Brandeis, T. A., & Sherrill, K. R. (2008). Mapping land cover and estimating forest structure using satellite imagery and coarse resolution lidar in the Virgin Islands. *Journal of Applied Remote Sensing*, *2*(1), doi:10.1117/1.3063939.

Khatami, R., & Mountrakis, G. (2012). Implications of classification of methodological decisions in flooding analysis from Hurricane Katrina. *Remote Sensing, 4*(12), 3877–3891.

Lu, D., & Weng, Q. (2007). A survey of image classification methods and techniques for improving classification performance. *International Journal of Remote Sensing, 28*(5), 823–870.

Luo, L., & Mountrakis, G. (2011). Converting local spectral and spatial information from a priori classifiers into contextual knowledge for impervious surface classification. *ISPRS Journal of Photogrammetry and Remote Sensing, 66*(5), 579–587.

Mantero, P., Moser, G., & Serpico, S. B. (2005). Partially supervised classification of remote sensing images through SVM-based probability density estimation. *IEEE Transactions on Geoscience and Remote Sensing, 43*(3), 559–570.

Martinuzzi, S., Vierling, L. A., Gould, W. A., Vierling, K. T., & Hudak, A. T. (2009). Incorporating remotely sensed tree canopy cover data into broad scale assessments of wildlife habitat distribution and conservation. *Journal of Applied Remote Sensing*, *3*(1), doi:10.1117/1.3279080.

Mohammady, M., Moradi, H. R., Zeinivand, H., & Temme, A. (2015). A comparison of supervised, unsupervised and synthetic land use classification methods in the north of Iran. *International Journal of Environmental Science and Technology, 12*(5), 1515–1526.

Mohammdy, M., Moradi, H. R., Zeinivand, H., Temme, A. J. A. M., Pourghasemi, H. R., & Alizadeh, H. (2014). Validating gap-filling of Landsat ETM+ satellite images in the Golestan Province, Iran. *Arabian Journal of Geosciences, 7*, 3633–3638.

Mountrakis, G., & Luo, L. (2011). Enhancing and replacing spectral information with intermediate structural inputs: a case study on impervious surface detection. *Remote Sensing of Environment, 115*(5), 1162–1170.

Mountrakis, G., Im, J., & Ogole, C. (2011). Support vector machines in remote sensing: a review. *ISPRS Journal of Photogrammetry and Remote Sensing, 66*(3), 247–259.

Neuenschwander, A. L., Magruder, L. A., & Tyler, M. (2009). Land cover classification of small-footprint, full-waveform lidar data. *Journal of Applied Remote Sensing*, *3*(1), doi:10.1117/1.3229944.

Núñez, L., Grosjean, M., & Cartajena, I. (2002). Human occupations and climate change in the Puna de Atacama, Chile. *Science, 298*(5594), 821–824.

Oommen, T., Misra, D., Twarakavi, N. K. C., Prakash, A., Sahoo, B., & Bandopadhyay, S. (2008). An objective analysis of support vector machine based classification for remote sensing. *Mathematical Geosciences, 40*(4), 409–424.

Pfanzagl, J. (1994). Parametric statistical theory. Hamböker. Berlin, DE: Walter de Gruyter. 207–208.

Richards, J. A., & Jia, X. (2006). Remote sensing digital image analysis: an introduction. *Remote Sensing Digital Image Analysis: An Introduction*, 1-439.

Sen, G., Bayramoglu, M. M., & Toksoy, D. (2015). Spatiotemporal changes of land use patterns in high mountain areas of Northeast Turkey: a case study in Maçka. *Environmental Monitoring and Assessment, 187*(8), 1–14.

Shaw, S. B., Marrs, J., Bhattarai, N., & Quackenbush, L. (2014). Longitudinal study of the impacts of land cover change on hydrologic response in four mesoscale watersheds in New York State, USA. *Journal of Hydrology*, 519(PA), 12–22.

Skizadeh, M. (2015). Assessment the performance of classification methods in water quality studies, a case study in Karaj River. *Environmental Monitoring and Assessment, 187*(9), 1–12.

Soffianian, A., & Madanian, M. (2015). Monitoring land cover changes in Isfahan Province, Iran using Landsat satellite data. *Environmental Monitoring and Assessment, 187*(8), 1–15.

Stehman, S. V. (1997). Selecting and interpreting measures of thematic classification accuracy. *Remote Sensing of Environment, 62*(1), 77–89.

Szuster, B. W., Chen, Q., & Borger, M. (2011). A comparison of classification techniques to support land cover and land use analysis in tropical coastal zones. *Applied Geography, 31*(2), 525–532.

USGS, (2004). Phase 2 gap-fill algorithm: SLC-off gap-filled products gap-fill algorithm methodology. Available online at landsat.usgs.gov/documents/L7SLCGapFilledMethod.pdf. Accessed 28 Nov 2010.

Van Der Linden, S., Janz, A., Waske, B., Eiden, M., & Hostert, P. (2007). Classifying segmented hyperspectral data from a heterogeneous urban environment using support vector machines. *Journal of Applied Remote Sensing*, *1*(1), doi: 10.1117/1.2813466.

Vörösmarty, C. J., Green, P., Salisbury, J., & Lammers, R. B. (2000). Global water resources: vulnerability from climate change and population growth. *Science, 289*(5477), 284–288.

Vorovencii, I. (2014a). A change vector analysis technique for monitoring land cover changes in Copsa Mica, Romania, in the period 1985–2011. *Environmental Monitoring and Assessment, 186*(9), 5951–5968.

Vorovencii, I. (2014b). Assessment of some remote sensing techniques used to detect land use/land cover changes in South-East Transilvania, Romania. *Environmental Monitoring and Assessment, 186*(5), 2685–2699.

Walker, N. J., & Schulze, R. E. (2008). Climate change impacts on agro-ecosystem sustainability across three climate regions in the maize belt of South Africa. *Agriculture, Ecosystems and Environment, 124*(1–2), 114–124.

Wang, Z.-J., Jiao, J.-Y., Lei, B., & Su, Y. (2015). An approach for detecting five typical vegetation types on the Chinese Loess Plateau using Landsat TM data. *Environmental Monitoring and Assessment, 187*(9), 1–16.

Wentz, E. A., Stefanov, W. L., Gries, C., & Hope, D. (2006). Land use and land cover mapping from diverse data sources for an arid urban environments. *Computers, Environment and Urban Systems, 30*(3), 320–346.

Xing, E. P., Ng, A. Y., Jordan, M. I., & Russell, S. (2003). Distance metric learning, with application to clustering with side-information. *Advances in Neural Information Processing Systems*, 505–512.

Zhang, Y., Huang, D., Ji, M., & Xie, F. (2011). Image segmentation using PSO and PCM with Mahalanobis distance. *Expert Systems with Applications, 38*(7), 9036–9040.